RAYMENT, I., BAKER, T. S. & CASPAR, D. L. D. (1983). *Acta Cryst.* B39, 505-516.
RAYMENT, I., BAKER, T. S., CASPAR, D. L. D. & MURAKAMI, W. T. (1982). *Nature (London)*, **295**, 110-115.
ROSSMANN, M. G. (1990). *Acta Cryst.* A46, 73-82.
ROSSMANN, M. G., ARNOLD, E., ERICKSON, J. W., FRANKENBERGER, E. A., GRIFFITH, J. P., HECHT, H. J., JOHNSON, J. E., KAMER, G., LUO, M., MOSSER, A. G., RUECKERT, R. R., SHERRY, B. & VRIEND, G. (1985). *Nature (London)*, **317**, 145-153.
ROSSMANN, M. G. & BLOW, D. M. (1962). *Acta Cryst.* **15**, 24-31.
ROSSMANN, M. G. & JOHNSON, J. E. (1989). *Annu. Rev. Biochem.* **58**, 533-573.
SCHMIDT, T., JOHNSON, J. E. & PHILLIPS, W. E. (1983). *Virology*, **127**, 65-73.
SMITH, M. H. (1968). In *Handbook of Biochemistry, Selected Data for Molecular Biology*, edited by H. A. SOBER, pp. C-28-C-35. Cleveland: CRC Press.
TSAO, J. (1990). PhD thesis, Purdue Univ., West Lafayette, Indiana, USA.
TSAO, J., CHAPMAN, M. S., AGBANDJE, M., KELLER, W., SMITH, K., WU, H., LUO, M., SMITH, T. J., ROSSMANN, M. G., COMPANS, R W. & PARRISH, C. R. (1991). *Science* **251**, 1456-1464.
TSAO, J., CHAPMAN, M. S. & ROSSMANN, M. G. (1992). *Acta Cryst.* A48, 293-301.
TSAO, J., CHAPMAN, M. S., WU, H., AGBANDJE, M., KELLER, W. & ROSSMANN, M. G. (1992). *Acta Cryst.* B48, 75-88.
VALEGÅRD, K., LILJAS, L., FRIDBORG, K. & UNGE, T. (1990). *Nature (London)*, **345**, 36-41.
WOBBE, C. R., MITRA, S. & RAMAKRISHNAN, V. (1984). *Biochemistry*, **23**, 6565-6569.

Acta Cryst. (1992). A48, 312-322

Some Applications of the Phased Translation Function in Macromolecular Structure Determination

BY G. A. BENTLEY AND A. HOUDUSSE

Unité d'Immunologie Structurale (CNRS URA 359), Institut Pasteur, 25 rue du Dr Roux, Paris 75724, France

(*Received* 14 *February* 1991; *accepted* 5 *November* 1991)

Abstract

Although the phased translation function was first described some time ago [Colman, Fehlhammer & Bartels (1976). In *Crystallographic Computing Techniques*, edited by F. R. Ahmed, K. Huml & B. Sedláček, pp. 248-258. Copenhagen: Munksgaard], it has been little used, especially in the application of molecular replacement to macromolocular structures. Nevertheless, the procedure is relatively easy to apply and deserves wider use. In this paper the versatility of the phased translation function in a number of different applications is examined and experience gained in obtaining optimal results in protein structure determination by this method is reported. Examples given show how it can be used to position an oriented fragment, to locate independent components with respect to a common crystallographic origin and to choose correctly between enantiomorphic space groups. Its performance is compared with other translation functions in common use.

1. Introduction

Molecular replacement is widely used to determine macromolecular structures since there now exists a large resource of known structures which may contain one or more examples closely homologous to the molecule under study. The method proceeds in two stages. Firstly, the homologous molecule of known structure, or a fragment of it, is oriented in the unit cell of the unknown structure by means of a rotation function. Secondly, the correctly oriented homologue is positioned with respect to a crystallographic origin using a translation function, providing an initial model of the unknown crystal structure for further refinement. Whereas the rotation functions in current use exploit properties of the Patterson function (Rossmann & Blow, 1962; Huber, 1965; Crowther, 1972), translation functions may use the Patterson function (Crowther & Blow, 1967; Harada, Lifchitz, Berthou & Jolles, 1981), the correlation between the observed and calculated structure amplitudes, as in the *R*-factor search (Taylor & Morley, 1959; Fujinaga & Read, 1987), or phased structure amplitudes, as in the phased translation function (Colman, Fehlhammer & Bartels, 1976; Doesburg & Beurskens, 1983; Read & Schierbeek, 1988; Cygler & Desrochers, 1989).

We have used the phased translation function (PTF) to aid the solution of two crystal structures of Fab fragments by molecular replacement: the complex FabD1.3-FabE225 (Bentley, Boulot, Riottot & Poljak, 1990) and FabE5.2 (Houdusse, Bentley, Boulot, Eiselé & Poljak, unpublished results). Although we used it primarily to locate independent components with respect to a common origin, we performed additional calculations to test its general

0108-7673/92/030312-11$03.00

utility. This paper reports some of this experience and discusses the use of the PTF to resolve certain problems that may arise in the application of molecular replacement to protein structure determination. To this end, we also include test calculations performed with the antibody fragment FvD1.3 (Bhat, Bentley, Fischmann, Boulot & Poljak, 1990) which had already been solved by molecular replacement. In particular, we compare this approach with other methods commonly used to solve the translation problem.

2. The phased translation function

The mathematical basis of the PTF has been described elsewhere (Colman, Fehlhammer & Bartels, 1976; Doesburg & Beurskens, 1983; Read & Schierbeek, 1988). The principle of the function is best visualized in real space. The electron density of the model homologous structure, correctly oriented by the rotation function, is arbitrarily positioned in a unit cell with symmetry $P1$ but with the dimensions and angles of the unknown crystal form. The model electron density is then translated at regular grid intervals over the electron density of the unknown structure obtained, for example, by isomorphous replacement or by using calculated phases from a partial structure. At each grid point, $\mathbf{t}$, the integral, $S(\mathbf{t})$, of the superimposed electron densities is calculated,

$$S(\mathbf{t}) = \int_V \rho(\mathbf{x})\rho_{\text{model}}(\mathbf{x}-\mathbf{t})\,\mathrm{d}\mathbf{x} \qquad (1)$$

where ρ and ρ_{model} are the densities of the unknown crystal structure and the model structure respectively. Since ρ_{model} contains one orientation only (*i.e.* has symmetry $P1$), the volume of integration, V, is the complete unit cell. The maximum of $S(\mathbf{t})$ corresponds to the optimum superposition of the known structure onto the unknown structure and its coordinates thus give the required vector translation of the model for correct positioning in the unit cell. While the calculation of $S(\mathbf{t})$ may be performed in direct space, it may also be calculated in reciprocal space as a Fourier summation,

$$S(\mathbf{t}) = (1/V)\sum_{\mathbf{h}} \mathbf{F}(\mathbf{h})\mathbf{F}^*_{\text{model}}(\mathbf{h}) \exp(-2\pi i\mathbf{h}.\mathbf{t}) \qquad (2)$$

where $\mathbf{F}(\mathbf{h})$ and $\mathbf{F}_{\text{model}}(\mathbf{h})$ are the structure factors of ρ and ρ_{model} respectively. Since $\mathbf{F}_{\text{model}}(\mathbf{h})$ has $P1$ symmetry, the summation is performed over the whole of reciprocal space and the structure factors, $\mathbf{F}(\mathbf{h})$, must be expanded accordingly.

The successful application of the PTF has been reported for a small number of protein structures solved by molecular replacement. In these examples, phases of the structure factors of the unknown molecule were provided either by isomorphous replacement at low resolution, where the electron density maps had not been interpreted (Colman, Deisenhofer, Huber & Palm, 1976; Schierbeek *et al.*, 1989; Bentley *et al.*, 1990), or by calculated phases from partial models (Cygler & Anderson, 1988*b*; Cygler & Desrochers, 1989).

The use of the PTF with calculated phases from partial structures was described by Doesburg & Beurskens (1983), who applied the method to small molecules. The oriented model is at first arbitrarily positioned in the unit cell. The observed structure amplitudes are then expanded by crystal symmetry to $P1$ and phased by this molecule alone (*i.e.* molecules generated by the space-group symmetry were not included), providing the structure factors, $\mathbf{F}(\mathbf{h})$, for (2). The electron density map calculated from these structure factors thus contains not only the oriented model used for phasing but also its symmetry components related to the origin whose position is to be determined. These symmetry-related components will, of course, appear with a lower weight in the electron density map. If they can be located, the positions of the symmetry elements may then be deduced and the translation problem is solved. This is achieved as follows. A space-group symmetry operation is applied to the arbitrarily placed but correctly oriented model. This is used as a search model by providing the calculated structure factors, $\mathbf{F}_{\text{model}}(\mathbf{h})$, for (2). If A is the rotation matrix of this symmetry operation, I is the identity matrix, $\mathbf{t}_0$ is the position of the maximum in the resulting PTF and $\mathbf{q}_0$ is the required translation to place the molecule correctly in the unit cell (*i.e.* that used to phase the observed structure factors), then

$$(\mathbf{A}-\mathbf{I})\mathbf{q}_0 = \mathbf{t}_0 \qquad (3)$$

It is assumed in this equation that the phasing component is described by the symmetry position (x, y, z). Certain components of $\mathbf{q}_0$ may remain undetermined for a given choice of symmetry operation since the matrix $(\mathbf{A}-\mathbf{I})$ is singular for rotation axes and mirror planes. Thus, more than one symmetry position must be used to obtain a complete solution to the translation for many space groups. In practice, Doesburg & Beurskens (1983) used difference coefficients, $(F_{\text{obs}} - F_{\text{calc}}) \exp(2\pi i\alpha_{\text{calc}})$, to remove the contribution of the phasing model. These coefficients, containing information essentially on the symmetry-related molecules only, are thus used as $\mathbf{F}(\mathbf{h})$ in (2). They found this approach to be reliable for small molecules provided the oriented model represented 10% or more of the total diffracting power of the unit cell.

The use of the PTF with calculated phases has been successfully applied to protein structures by Cygler & Anderson (1988*b*). Unlike Doesburg & Beurskens (1983), however, they performed the calculation in direct space rather than in reciprocal space, removing the density of the phasing model with a molecular envelope. Their procedure was expensive in computing time, but they obtained good results, even with

the phasing component representing only 10–15% of the unit-cell contents. In a more recent development of this direct-space procedure, Cygler & Desrochers (1989) describe a full-symmetry translation function where the results from all symmetry elements are combined to optimize the signal. They also succeeded in greatly reducing computing time.

The Patterson-based translation function and the PTF using phases calculated from partial models are formally close to one another. Thus, if we first consider just two symmetry operations, k and l, it may be shown that

(a) for the Patterson method (see Tickle, 1985),

$$\begin{aligned} T_{\text{Patterson}}(\mathbf{t}) = \sum_{\mathbf{h}} \{F_{\text{obs}}(\mathbf{h})^2 - \sum_{m} [F'_{\text{calc}}(A_m^*\mathbf{h})]^2\} \\ \times F'_{\text{calc}}(A_k^*\mathbf{h}) F'_{\text{calc}}(A_l^*\mathbf{h}) \\ \times \exp\{i[\varphi'(A_k^*\mathbf{h}) - \varphi'(A_l^*\mathbf{h})] \\ + 2\pi i \mathbf{h}\cdot(\mathbf{d}_k - \mathbf{d}_l)\} \\ \times \exp[2\pi i (A_k^* - A_l^*)\mathbf{h}\cdot\mathbf{t}]; \end{aligned} \tag{4}$$

(b) for the PTF (using difference coefficients to remove the contribution from the phasing model),

$$\begin{aligned} T_{\text{PTF}}(\mathbf{t}) &= \sum_{\mathbf{h}} [\mathrm{F}_{\text{obs}}(\mathbf{h}) - F'_{\text{calc}}(A_k^*\mathbf{h})] \\ &\quad \times \exp[i\varphi'(A_k^*\mathbf{h}) + 2\pi i \mathbf{h}\cdot(A_k\mathbf{t} + \mathbf{d}_k)] \\ &\quad \times F'_{\text{calc}}(A_l^*\mathbf{h}) \exp[-i\varphi'(A_l^*\mathbf{h}) \\ &\quad - 2\pi i \mathbf{h}\cdot(A_l\mathbf{t} + \mathbf{d}_l)] \\ &= \sum_{\mathbf{h}} \{[F_{\text{obs}}(\mathbf{h})/F'_{\text{calc}}(A_k^*\mathbf{h})] - 1\} \\ &\quad \times F'_{\text{calc}}(A_k^*\mathbf{h}) F'_{\text{calc}}(A_l^*\mathbf{h}) \\ &\quad \times \exp\{i[\varphi'(A_k^*\mathbf{h}) - \varphi'(A_l^*\mathbf{h})] \\ &\quad + 2\pi i \mathbf{h}\cdot(\mathbf{d}_k - \mathbf{d}_l)\} \\ &\quad \times \exp[2\pi i (A_k^* - A_l^*)\mathbf{h}\cdot\mathbf{t}]; \end{aligned} \tag{5}$$

A_i and $\mathbf{d}_i$ are the rotation matrix and translation vector respectively of the ith symmetry operator, F'_{calc} is the calculated partial structure amplitude for the symmetry position (x, y, z) with φ' being the corresponding phase, F_{obs} is the observed structure amplitude and $\mathbf{t}$ is the translation. Thus symmetry position k provides the phasing model, while symmetry position l provides the search model. The formulation of the PTF given by (5) differs from that given by (1) and (2); in the former, the phasing model and, consequently, the search model are moved with respect to an arbitrary origin while, in the latter, they remain fixed and the model electron density map is translated. Both formulations, however, are equivalent to one another. Equations (4) and (5) are thus identical except in the first component of the Fourier coefficient of the summation. Use of full symmetry in the Patterson-based function simply includes a summation of (4) over all pairs of symmetry operations k and l ($k < l$) (Tickle, 1985). We may also obtain, by introducing the same summation in (5), a full symmetry PTF in much the same manner as did Cygler & Desrochers (1989) for their direct-space procedure,

$$\begin{aligned} T_{\text{PTF}}(\mathbf{t}) = \sum_{\mathbf{h}} \Bigg(\sum_{\substack{k \\ k<l}} \sum_{l} \{[F_{\text{obs}}(\mathbf{h})/F'_{\text{calc}}(A_k^*\mathbf{h})] - 1\} \\ \times F'_{\text{calc}}(A_k^*\mathbf{h}) F'_{\text{calc}}(A_l^*\mathbf{h}) \\ \times \exp\{i[\varphi'(A_k^*\mathbf{h}) - \varphi'(A_l^*\mathbf{h})] \\ + 2\pi i \mathbf{h}\cdot(\mathbf{d}_k - \mathbf{d}_l)\} \\ \times \exp[2\pi i (A_k^* - A_l^*)\mathbf{h}\cdot\mathbf{t}] \Bigg). \end{aligned} \tag{6}$$

In the following paragraphs we describe the use of both calculated phases from partial structures and isomorphous replacement phases in the application of the PTF in its reciprocal-space formulation to protein structure determination. Because of previous work on the PTF, which we have referred to above, our emphasis is on those aspects relating to the use of calculated phases. We have used the function in the full symmetry calculation [(6)] for comparison. We have tried removal of contributions from the

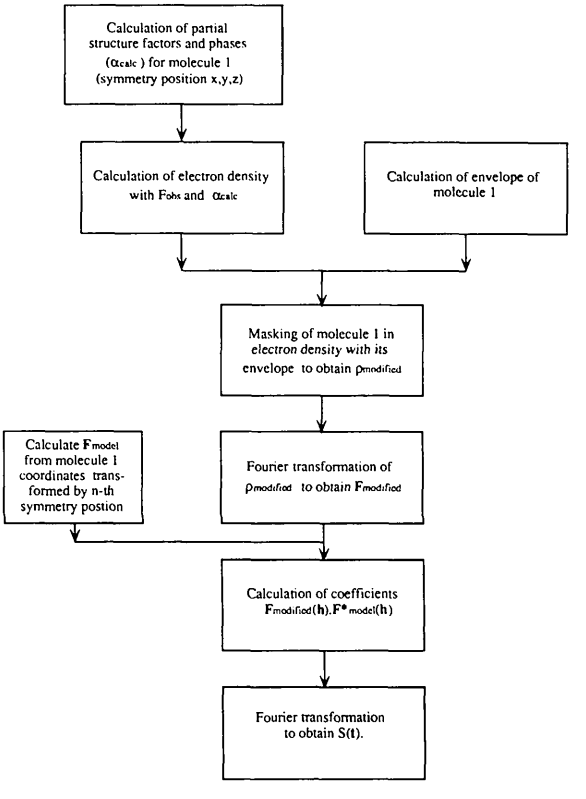

Fig. 1. Flow diagram for PTF in reciprocal space with elimination of phasing density by a molecular envelope.

phasing model both by difference coefficients and molecular envelopes. The protocol used when masking the electron density of the phasing model is shown in Fig. 1. We begin with examples using the PTF to determine the translation of an oriented molecule or fragment to locate it correctly in the unit cell. This is followed with examples showing its use in determining the translation required to locate an oriented component with respect to a crystallographic origin defined already by another component in the unit cell or by isomorphous replacement phases. The performance of the PTF is compared with other commonly used translation functions.

3. Materials

3.1. *Programs*

Rotation-function calculations were made with the program *ROTFUN* written by Navaza (1987). Programs for other translation functions used include *SEARCH* (SERC Daresbury Laboratory, 1986) for *R*-factor or correlation-coefficient searches (correlation between observed and calculated structure amplitudes) and *TFSGEN* (Tickle, 1985) for a Patterson-based method (Harada *et al.*, 1981). Programs used for Fourier and structure-factor calculations and file manipulations were taken from the *CCP*4 suite (SERC Daresbury Laboratory, 1986). Comparisons with the PTF in direct space were made with the program *RTRANS* kindly provided by Drs Cygler and Desrochers. The full-symmetry PTF in its reciprocal-space formulation [(6)] was performed using a modified version of the program *TFSGEN* (program *SYMPTF*).

3.2. *Introduction to structures used*

The structures used for our calculations were antigen-binding fragments (Fab and Fv) of antibody molecules. An Fab molecule is composed of a heavy (H) and a light (L) polypeptide chain and has, in total, four domains: V_H, V_L, C_H1 and C_L. Although the pairs V_H/V_L (variable dimer, Fv) and C_H1/C_L (constant dimer) associate by strong non-covalent interactions (C_H1 and C_L are, however, connected by a disulfide bridge), the connection between V_H and C_H1 and between V_L and C_L is maintained essentially by a flexible peptide link. Thus, while the quaternary structure of the variable dimer and the constant dimer may each separately be quite well conserved between different Fab structures, the relative orientation between them, described by the elbow angle, is highly variable. The search model for an Fab molecule using the molecular replacement technique therefore requires two independent components: the variable and the constant dimers (Cygler & Anderson, 1988*a*).

3.2(i) *FabE*225-*FabD*1.3 *complex.* E225 is a monoclonal antibody (IgG2b, κ) that recognizes an idiotope on the monoclonal anti-lysozyme antibody D1.3 (IgG1, κ) (Amit, Mariuzza, Phillips & Poljak, 1986). The complex, FabD1.3-FabE225, formed between the antigen-binding fragments of these two antibodies, crystallizes in the space group $P2_1$ (a = 75.1, b = 77.7, c = 96.8 Å, β = 111.8°) with one molecule of complex (2 Fabs) in the asymmetric unit (Boulot *et al.*, 1987). Thus, four independent components must be oriented and positioned in the asymmetric unit: two dimers of each kind. The unrefined structure of FabD1.3 (Amit *et al.*, 1986), as seen in the complex with hen egg-white lysozyme, FabD1.3-HEL, provided initial models for both variable and constant dimers. The rotation function was calculated using the program *ROTFUN*; data between the resolution limits of 10 and 4 Å were included in the calculation and the lower and upper radial limits of integration in Patterson space were 4.5 and 25 Å respectively. Correct solutions for the variable dimers were first and third peaks of the rotation function (the second peak arose from the approximate twofold symmetry of the variable dimer from the first solution), while those for the constant dimers were given by the first and twelfth peaks. Each of these solutions gave peaks in the Patterson-based translation-function maps calculated with the program *TFSGEN*. This located each of the four components separately with respect to a crystallographic origin. The remaining task was to relate each of these solutions to a common origin. In the polar space group $P2_1$, the choice of origin in directions **x** and **z** is restricted to 0 or $\frac{1}{2}$; the choice in direction **y**, however, is arbitrary. Although the result of the translation function for one component may be used to fix an origin, additional information is required to locate the other three components with respect to the same origin. This was provided by the PTF using isomorphous phases. The crystal structure has been refined to 2.5 Å resolution (Bentley *et al.*, 1990).

3.2(ii) *FabE*5.2. E5.2 is a monoclonal antibody (IgG1, κ) that also recognizes an idiotope on the antibody D1.3. The Fab fragment crystallizes in the space group $P2_1$ with unit-cell parameters a = 44.5, b = 157.8, c = 66.9 Å, β = 100.5°; there are two molecules in the asymmetric unit (Houdusse, Bentley, Boulot, Eiselé & Poljak, unpublished results). Therefore, two variable and two constant dimers must be oriented and positioned in the asymmetric unit. Model structures for molecular replacement were chosen from the refined structures of FabE225 and FabD1.3 (Bentley *et al.*, 1990; Fischmann *et al.*, 1991). Conditions for the rotation-function calculation were similar to those used for the FabD1.3-FabE225 complex. Solutions for the constant dimers were clearly given by the first two peaks of the rotation function, while those for the variable dimers were given by the first and third peaks. All four orientations gave very

clear maxima in the translation-function maps calculated with the program *TFSGEN*. As with FabE225-FabD1.3, the next stage was to locate each component with respect to a common origin. Since the space group is also $P2_1$, the same considerations apply. All components were positioned with respect to a common origin using phases from partial calculated structure factors in the PTF in its reciprocal-space form. Refinement of the crystal structure at 2.6 Å resolution is currently in progress.

3.2(iii) *FvD*1.3. FvD1.3 consists of the V_H and V_L domains of the monoclonal antibody, D1.3, associated as a dimer by non-covalent interactions. It has been cloned into *E. coli* and expressed in quantities sufficient to achieve successful crystallizations (Boulot *et al.*, 1990). The space group is $P4_32_12$ with $a=90.6$, $c=56.4$ Å and there is one molecule of FvD1.3 per asymmetric unit. The structure had been readily solved by molecular replacement using the refined atomic coordinates (Fischmann *et al.*, 1991) of the variable dimer of FabD1.3-HEL. The rotation and translation functions were calculated with the programs *ROTFUN* and *TFSGEN*, respectively, employing similar conditions to those described for FabE225-FabD1.3. The translation function showed the space group to be $P4_32_12$ and not its enantiomorph, $P4_12_12$. The structure has been refined at 1.9 Å resolution (Bhat *et al.*, 1990). Although the initial model coordinates for FvD1.3 were provided by the refined FabD1.3-HEL structure, the final refined model of the Fv fragment showed a difference in relative orientation between V_L and V_H of about 3°. Calculations with the PTF were made to test its performance against the Patterson-based translation function.

4. Applications

These structures were used to perform three series of trials of the PTF in reciprocal space.

(i) In each of the three crystal structures given above, the individual components (*i.e.* dimers) were located separately with respect to a crystallographic origin using phases from partial calculated structure factors. This was achieved by locating symmetry-related molecules (or the symmetry elements of the unit cell) as described in §2.

(ii) The function was used to locate the independently positioned components of the FabE225-FabD1.3 and FabE5.2 structures with respect to a common origin, again using phases from partial calculated structure factors. (This was not done for FvD1.3, which has one dimer per asymmetric unit.)

(iii) For FabE225-FabD1.3, individual dimers were located in the unit cell by the PTF calculated with isomorphous phases. (No isomorphous data were available for the other two structures.)

These are described successively in the three following subsections.

4.1. *Search for symmetry elements with the phased translation function*

The PTF was calculated in reciprocal space as outlined above. Models of the Fab dimers were first correctly oriented but arbitrarily positioned in the unit cell. As described in §2, the models were first used to phase the observed structure amplitudes which had been expanded by crystal symmetry to $P1$. Contributions from the phasing models to the calculated structure factors were removed by one of two procedures:

(*a*) The difference coefficients $(F_{obs}-F_{calc})\times \exp(2\pi i\alpha_{calc})$ were substituted for $\mathbf{F}(\mathbf{h})$ in (2). The scale factor between F_{obs} and F_{calc} was estimated by making a least-squares fit of $\langle F_{obs}\rangle$ to $\langle F_{calc}\rangle$ as a function of resolution. Even though only a small portion of the unit-cell contents was included in F_{calc} ($\sim\frac{1}{8}$ of the unit cell for all three examples), it was found empirically that this scale factor, rather than some fraction of it, gave the best results. This gave, in fact, a difference map with the smallest root-mean-square (r.m.s.) density and was without large peaks or troughs at the site of the phasing model. We tried using weights calculated by the procedure of Read (1986) but this did not show any improvement over unweighted coefficients; however, this method for obtaining weights may be inappropriate when such a small fraction of the unit cell is used to calculate the structure factors.

(*b*) The electron density of the phasing model in an F_{obs}, α_{calc} Fourier map was masked out with a molecular envelope. The envelope was constructed on a three-dimensional grid directly from the atomic coordinates of the phasing model. The results of the PTF proved to be rather insensitive to the value of the constant density placed inside the envelope, but optimum results were obtained when this was close to zero. The electron density thus modified was then transformed by inverse Fourier summation to obtain coefficients corresponding to $\mathbf{F}(\mathbf{h})$ in (2).

The structure factors corresponding to $\mathbf{F}_{model}(\mathbf{h})$ were calculated in $P1$ symmetry from the coordinates of the same model after transformation by one of the space-group symmetry operations. The PTF was then obtained as a Fourier summation using $\mathbf{F}(\mathbf{h})\mathbf{F}_{model}(\mathbf{h})^*$ as coefficients.

4.1(i) *FabD*1.3-*FabE*225 *and FabE*5.2. Results of the PTF in reciprocal space as well as the other translation functions described in §3.1 are presented for both FabD1.3-FabE225 and E5.2 in Table 1. All calculations described here were performed in the

Table 1. *Comparison of translation functions using FabD1.3-FabE225 and FabE5.2*

D1.3v, D1.3c and E225v, E225c denote the variable and constant dimers of FabD1.3 and FabE225 respectively. E5.2v and E5.2c denote the variable and constant dimers of FabE5.2 respectively; the molecule number in the asymmetric unit is given in parentheses. All trials shown here were made using diffraction data in the resolution range 20–3.5 Å. Peak heights are expressed in terms of the r.m.s. value of the translation function. The signal-to-noise ratio is given in parentheses, followed by the rank in height of the correct peak. (*a*) PTF calculated in reciprocal space using molecular envelopes to mask density from phasing model. See Fig. 1 for protocol. (*b*) PTF as in (*a*) using the final refined coordinates. (*c*) PTF calculated in direct space using *RTRANS*. (*d*) PTF calculated in reciprocal space using *SYMPTF*. (*e*) Patterson-based translation function using *TFSGEN*. (*f*) Correlation-coefficient search using *SEARCH*.

Dimer	(*a*) PTF	(*b*) PTF	(*c*) *RTRANS*	(*d*) *SYMPTF*	(*e*) *TFSGEN*	(*f*) *SEARCH*
D1.3v	12.6 (2.6) 1	17.8 (5.7) 1	4.1 (2.7) 1	11.2 (3.0) 1	10.4 (2.9) 1	10.6 (3.4) 1
D1.3c	8.2 (1.7) 1	8.8 (1.9) 1	3.1 (1.1) 1	4.8 (1.2) 1	6.0 (1.8) 1	4.7 (1.6) 1
E225v	8.8 (1.7) 1	20.1 (3.9) 1	2.0 (1.1) 1	6.0 (1.8) 1	6.8 (1.9) 1	6.2 (1.8) 1
E225c	4.3 (0.9) 5	10.4 (2.2) 1	2.6 (1.0) 1	2.8 (0.8) 6	3.8 (0.9) 2	4.0 (1.1) 1
E5.2v	7.7 (1.8) 1	12.8 (2.5) 1	4.6 (1.3) 1	5.3 (1.4) 1	6.9 (2.2) 1	5.7 (2.2) 1
E5.2c(1)	10.0 (2.0) 1	13.3 (2.6) 1	8.3 (2.3) 1	7.2 (2.4) 1	7.9 (2.3) 1	7.4 (2.6) 1
E5.2v(2)	5.9 (1.2) 1	12.3 (2.5) 1	5.8 (1.5) 1	4.9 (1.4) 1	4.8 (1.7) 1	5.7 (2.0) 1
E5.2c	6.0 (1.3) 1	10.3 (2.0) 1	5.1 (1.3) 1	6.6 (1.7) 1	7.5 (2.5) 1	6.6 (2.1) 1
$\langle S/N \rangle$*	1.6	2.9	1.5	1.7	2.0	2.1

* Average signal-to-noise ratio for each column.

resolution range of 20–3.5 Å. For the space group $P2_1$, it follows from (3) that if $(t_x, 0, t_z)$ are the coordinates of the correct peak in the PTF, then the required translation to place the phasing model correctly in the unit cell is $(-\frac{1}{2}t_x, 0, -\frac{1}{2}t_z)$. (The choice of y coordinate of a single dimer is arbitrary if considered on its own.) The results of the PTF for the FabE225-FabD1.3 complex and FabE5.2, expressed as peak height in r.m.s. units for the correct solution, are given in column (*a*) of Table 1. For both structures, contributions from the phasing models were removed using difference coefficients and molecular envelopes although only the results for the latter are shown since the two procedures produced similar values. The performance of the PTF using refined coordinates of FabE225-FabD1.3 are shown in column (*b*) for comparison. Our protocol for the PTF in reciprocal space (Fig. 1) was compared with the PTF in direct space using *RTRANS* (column *c*), the PTF in reciprocal space using *SYMPTF* (column *d*), the Patterson-based approach using *TFSGEN* (column *e*) and the correlation coefficient search with *SEARCH* (column *f*).

For space group $P2_1$, our reciprocal-space protocol, the *SYMPTF* procedure and the direct-space *RTRANS* procedure are all, in principle, equivalent since there are only two symmetry positions. Although each procedure gives approximately the same performance, as judged by the signal-to-noise (S/N) ratio† averaged over all dimers, it is interesting to note the variation in the S/N ratio of a given dimer for the three methods of calculation (Table 1). Since the observed diffraction data and the model structures are the same in each case, these differences must arise from the different methods of computing the translation function. *TFSGEN* and *SEARCH* performed equally well and produced the best results for these two crystal structures. We also draw attention to the difference in performance by *TFSGEN* and *SYMPTF*, given their similar bases [(4) and (5) respectively].

† *I.e.* the ratio of the height of the correct peak to that of the largest spurious peak.

Table 2. *Phased translation function in reciprocal space (PTF) and direct space (RTRANS) for FvD1.3*

The translation vector was calculated using equation (3). The height of the correct peak (always the highest in this example) followed by the signal-to-noise ratio are given for both translation functions. Peak heights are expressed in terms of the r.m.s. value of the translation function.

Equivalent position of search component	Translation vector (q_x, q_y, q_z)	PTF peak height	*RTRANS* peak height
$-x, -y, z+\frac{1}{2}$	(0.604, 0.589, -)	12.5 (2.3)	5.1 (1.3)
$-y+\frac{1}{2}, x+\frac{1}{2}, z+\frac{3}{4}$	(0.603, 0.589, -)	10.3 (1.8)	-
$y+\frac{1}{2}, -x+\frac{1}{2}, z+\frac{1}{4}$	(0.602, 0.591, -)	11.0 (2.3)	-
$-x+\frac{1}{2}, y+\frac{1}{2}, -z+\frac{3}{4}$	(0.603, - , 0.803)	11.4 (2.2)	7.3 (1.9)
$x+\frac{1}{2}, -y+\frac{1}{2}, -z+\frac{1}{4}$	(- , 0.588, 0.804)	10.5 (2.1)	7.4 (2.0)
$y, x, -z$	(- , - , 0.792)	10.4 (2.1)	-
$-y, -x, -z+\frac{1}{2}$	(- , - , 0.796)	11.2 (2.1)	-
Combined*	(0.600, 0.587, 0.806)	-	12.2 (1.8)

* Result from combining the three symmetry operations in *RTRANS*. See text for comparisons with *TFSGEN* and *SYMPF*.

4.1(ii) *FvD1.3*. Results of the PTF for FvD1.3, using data between 20 and 3.5 Å resolution are shown in Table 2. The phasing component was assigned to the symmetry position (x, y, z) and the search component was generated by the symmetry position indicated in the first column of the table. For these trials, contributions from the phasing model were removed by using both difference coefficients and molecular envelopes but, again, only the results of the latter are shown because of their similar performance. The third and fourth columns give the peak heights for the reciprocal-space PTF and *RTRANS* respectively. In

all instances, the correct peak was the highest. The translation (q_x, q_y, q_z), as deduced from (3), is given for each symmetry position in the second column; those coordinates left blank are indeterminate. As may be seen, at least two suitably chosen runs of the PTF must be performed to obtain a complete solution, but of course all combinations should be exploited to obtain maximum benefit. Although *RTRANS* provides a means for combining the results from all symmetry operations, it only deals with those symmetry axes parallel to crystallographic axes in its present form. Thus we show results for three symmetry operations only, both for the case where each is considered separately (which is equivalent to our reciprocal-space protocol) and for where they are combined. The full-symmetry calculation in reciprocal space with *SYMPTF* gave a comparable result to *RTRANS*, with the correct peak at (0.603, 0.589, 0.802) of height 14.6 r.m.s. units and a S/N ratio of 1.9. Unlike *RTRANS*, all symmetry positions were used in this calculation. Thus, the full-symmetry PTF calculations, whether in direct or reciprocal space, gave a result inferior to those where each symmetry operation was used separately. By way of comparison, the program *TFSGEN* (which also uses all symmetry positions) gave a similar result with the correct peak at height 17.4 r.m.s. units positioned at (0.602 0.590, 0.802) and a S/N ratio of 1.9. The correlation-coefficient search (program *SEARCH*) was not tested here because of the large computing time required to cover the asymmetric unit of this space group.

Trials of the PTF in reciprocal space were made using just the coordinates of the V_L domain of the FvD1.3 dimer, constituting about $\frac{1}{16}$ of the unit-cell contents, for calculating phases. In these runs, the contributions from the phasing components were removed by molecular envelopes. Although six of the seven runs gave the correct peak in first position (5.2–6.6 r.m.s. units), the second peak was always comparable in height. When difference coefficients were tried, the correct peaks, although identified from prior knowledge of their true positions, were not significant in height. Thus, removal of density from the phasing model with molecular envelopes gives cleaner results and their use may be essential when the model is only a small fraction of the unit-cell contents, or where it is poorer in structural homology to the unknown molecule. The performance of *TFSGEN* was notably superior to that using the PTF in this case, probably reflecting the advantage of using all eight symmetry positions; the correct peak was the maximum with a height of 9.2 r.m.s. units and a S/N ratio of 1.6.

By using those symmetry positions which distinguish $P4_32_12$ from $P4_12_12$, it was possible to choose the correct enantiomorphic space group or FvD1.3. For example, if the symmetry positions 3 and 4 in the *International Tables for X-ray Crystallography* (1974) (see rows 2 and 3 of Table 2) are chosen for generating the search component, then the true peak will occur at $z = 0$ for the correct enantiomorph and at $z = \frac{1}{2}$ for the incorrect choice; in each instance, the x and y coordinates and the peak height remain unchanged by the space group chosen for the calculation. The space group was clearly shown to be $P4_32_12$ by this criterion. The indication, in fact, was less ambiguous than the result given by *TFSGEN*. Since four of the symmetry positions are common to both enantiomorphs, a peak should occur at the correct position in both space groups by the latter method; the distinction must be made on height since it will be halved in magnitude for the incorrect choice. Accordingly, *TFSGEN* gave a peak of height 8.3 r.m.s. units (S/N ratio of 0.8) at the correct position, when calculated in $P4_12_12$. The same considerations apply to *SEARCH*. By using the appropriate symmetry positions in the PTF, however, the choice depended on the restricted values allowed for the z coordinate of the correct peak as well as its height.

4.2. *Search for a common origin for several components using partial calculated structure factors*

The particular problem posed by the crystal structures FabE225-FabD1.3 and FabE5.2 lies in positioning the independent components (four in both cases) with respect to a common origin in space group $P2_1$. As discussed at the beginning of this section, the biggest difficulty arises in determining the relative y coordinates of the dimers. Indeed, it was this problem which initially prompted us to use the PTF.

The procedure differs in some details to those given in the previous subsection. First, one of the oriented dimers was correctly positioned in the unit cell (using *TFSGEN*); this served to define a crystallographic origin. Phases calculated with this component, using the full space-group symmetry, were applied to the observed structure amplitudes, which were subsequently expanded by crystal symmetry to $P1$. Contributions from the phasing models were removed as outlined above to obtain the coefficients $\mathbf{F}(\mathbf{h})$ for (2). From the coordinates of the second oriented dimer, the structure factors $\mathbf{F}_{\text{model}}(\mathbf{h})$ were calculated in symmetry $P1$. The PTF thus gave the translation required to locate the second component correctly with respect to the origin defined by the first dimer.

Trials with FabD1.3–FabE225 were made for all possible combinations of dimers as phasing and search components. Results are given in Table 3. Columns (*a*) and (*b*) contain results using data in the resolution range of 20–6 and 20–3.5 Å respectively, employing molecular envelopes to remove contributions from the phasing model. Column (*c*) shows results from data in the resolution range 20–3.5 Å, using difference coefficients to remove contributions

from the phasing component. Finally, in column (*d*), we give results using the refined coordinates of the complex; the resolution range was also 20–3.5 Å and molecular envelopes were used to mask density from the phasing models. Peak heights are expressed in terms of the r.m.s. value of the function as described for Table 1. Comparison of columns (*a*) and (*b*) shows a clear advantage in using high-resolution data. The use of difference coefficients gave comparable results to those obtained by masking with molecular envelopes at high resolution only; at 6 Å resolution, difference coefficients were significantly inferior (data not shown).

The number of dimer pairs giving a clear maximum was sufficient to provide a model of the FabD1.3–FabE225 complex as well as to furnish a generous cross-checking for internal consistency of the dimer positions thus obtained. These peaks assembled the four components in the asymmetric unit such that each variable dimer matched a constant dimer to give the correct covalent linkage between the light and heavy polypeptide chains. The absence of unacceptable intermolecular contacts in the unit cell further confirmed that the correct solution for the complex had been obtained.

Similar trials were made with data from FabE5.2. This structure gave better results than the Fab–Fab complex, showing the benefit of more accurate model coordinates. The heights of the correct peaks ranged from 11.0 to 7.1 r.m.s. From these peak positions, a consistent model of two Fab molecules in the asymmetric unit could be constructed, providing a starting point for the refinement now in progress.

4.3. *Phased translation function with phases from isomorphous replacement*

Intensity data for two isomorphous derivatives of the FabE225–FabD1.3 complex, prepared from tripotassium pentafluorodioxouranate ($K_3F_5UO_2$) and tetrakis(acetoxymercurio)methane, were measured. These gave interpretable difference Patterson functions but subsequent heavy-atom parameter refinement and isomorphous phase determination showed a serious lack of isomorphism and phases were not used beyond 4 Å resolution (mean figure of merit was 0.53). The observed structure amplitudes, weighted by their figures of merit, and the isomorphous replacement phases were used to form the coefficients $\mathbf{F}(\mathbf{h})$ in (2). The crystallographic origin of reference was thus defined by the heavy-atom positions of the derivatives. Since the hand of the heavy-atom configuration was not known, both enantiomorphic sets of isomorphous phases were tried in the PTF. Partial structure factors for each of the oriented variable and constant dimers were calculated in symmetry *P*1 to provide the coefficients $\mathbf{F}_{\text{model}}$ in (2).

Table 3. *The search for a common origin for independent components: PTF of FabD1.3–FabE225 using partial calculated structure factors*

D1.3v, D1.3c, E225v and E225c are defined in Table 1. Columns (*a*), (*b*) and (*c*) are results using the initial unrefined coordinates; in (*d*) the refined structure was used. The density from the phasing component was removed by means of the mask for (*a*), (*b*) and (*d*) and by means of a difference map in (*c*). The resolution range of the data used for each set of trials is indicated at the head of each column. The results are shown as peak heights as in Table 1.

Phasing component	Search component	(*a*) 20–6 Å	(*b*) 20–3.5 Å	(*c*) 20–3.5 Å	(*d*) 20–3.5 Å
D1.3v	E225v	5.6 (1.2) 1	14.0 (1.2) 1	12.8 (2.7) 1	18.3 (3.9) 1
	E225c	5.8 (1.4) 1	10.2 (2.3) 1	8.2 (1.7) 1	13.2 (3.0) 1
	D1.3c	5.3 (1.3) 1	10.3 (2.1) 1	9.7 (2.3) 1	13.9 (3.4) 1
D1.3c	E225v	4.5 (0.9) 2	8.2 (1.9) 1	6.8 (1.5) 1	15.5 (3.2) 1
	E225c	3.3 (0.7) 19	5.8 (1.3) 1	5.6 (1.3) 1	10.3 (2.2) 1
	D1.3v	4.6 (1.1) 1	8.7 (1.8) 1	7.7 (1.6) 1	15.9 (3.6) 1
E225v	E225c	4.0 (0.9) 5	5.5 (1.3) 1	5.5 (1.4) 1	11.8 (2.0) 1
	D1.3v	3.9 (0.9) 5	11.3 (2.4) 1	10.2 (2.3) 1	21.3 (4.4) 1
	D1.3c	3.8 (0.8) 6	6.2 (1.3) 1	5.9 (1.4) 1	13.2 (3.1) 1
E225c	E225v	3.0 (0.8) 68	8.6 (1.9) 1	7.3 (1.5) 1	14.1 (3.1) 1
	D1.3v	4.8 (1.0) 2	9.3 (2.1) 1	8.8 (1.9) 1	17.9 (3.9) 1
	D1.3c	2.8 (0.7) 69	5.1 (1.1) 1	4.5 (0.9) 3	12.1 (2.6) 1

Table 4. *PTF using isomorphous phases of FabD1.3–FabE225*

D1.3v, D1.3c, E225v and E225c are defined in Table 1. The height of the correct peak (always the maximum of the function in this example) and the signal-to-noise ratio (given in parentheses) are shown for each search component. Peak heights are expressed in terms of the r.m.s. value of the function.

Search component	Resolution range 20–6 Å	20–4 Å
D1.3v	6.7 (1.8)	16.1 (3.4)
D1.3c	7.1 (1.3)	11.4 (2.9)
E225v	6.3 (1.7)	14.5 (3.1)
E225c	6.5 (1.7)	12.0 (2.9)

All four components gave clear peaks in the PTF, at positions consistent with those indicated by *TFSGEN*, for one choice of heavy-atom enantiomorph only. The results shown in Table 4 give, for each dimer, the heights of the true peak (always the maximum in this example) and the S/N ratio. From these peak positions, a consistent model of a complex of two Fabs could be constructed in the unit cell. As may be seen, the results are significantly better at 4 Å resolution than they are at 6 Å, in spite of the increased deviation from isomorphism at higher resolution. Phases from the other enantiomorph gave peaks of much lower weight (maximum observed was 5.3 r.m.s. units at 4 Å resolution) which were not consistent with the results of *TFSGEN* and from which no acceptable solution for the complex could be constructed. The application of the PTF as described here actually leads to the initial model used to refine this structure at 2.5 Å.

4.4. *Effect of errors in orientation*

We compared the sensitivity of the different translation functions to errors in orientation. In these tests,

Table 5. *Effect of orientation errors on translation functions for FabD1.3-FabE225*

Calculations made using data from the complex FabE225-FabD1.3 to place D1.3v in the unit cell. Peak heights are expressed as in Table 1. (*a*) Reciprocal-space PTF using isomorphous phases to 4 Å resolution. (*b*) Reciprocal-space PTF using calculated phases at 3.5 Å resolution. (*c*) Direct-space PTF (*RTRANS*) at 3.5 Å. (*d*) Patterson search (*TFSGEN*) at 3.5 Å resolution. (*e*) Correlation coefficient search (*SEARCH*) at 3.5 Å resolution.

Orientation error (°)	(*a*) PTF (iso)	(*b*) PTF (calc)	(*c*) *RTRANS*	(*d*) *TFSGEN*	(*e*) *SEARCH*
0	16.1 (3.4) 1	12.6 (2.6) 1	4.1 (2.7) 1	10.4 (2.9) 1	10.6 (3.2) 1
2	14.6 (3.0) 1	10.5 (2.1) 1	3.6 (2.4) 1	7.9 (1.7) 1	8.4 (2.8) 1
4	12.6 (2.4) 1	8.8 (1.8) 1	2.7 (1.5) 1	6.7 (1.6) 1	7.2 (2.3) 1
6	11.5 (2.3) 1	6.6 (1.1) 1	2.0 (1.1) 1	5.1 (1.1) 1	6.0 (1.8) 1
8	8.9 (1.6) 1	5.3 (1.0) 1	1.4 (0.9) 4	3.7 (0.8) 6	4.8 (1.5) 1
10	6.7 (1.5) 1	6.1 (1.1) 1	1.3 (0.9) 4	2.8 (0.6) 11	3.3 (1.0) 1
12	5.7 (1.2) 1	3.8 (0.7) 13	-	-	3.1 (0.8) 2
14	4.4 (0.9) 2	3.5 (0.7) 43	-	-	2.8 (0.7) 13

Table 6. *Effect of orientation errors on translation functions for FvD1.3*

All calculations were performed in the resolution range 20-3.5 Å using the unrefined coordinates of FvD1.3. Peak heights are expressed as for Table 1. (*a*) The Patterson-based method using *TFSGEN*. (*b*) The PTF reciprocal space following the protocol in Fig. 1. The phasing component was provided by the symmetry position (x, y, z) and the search component by symmetry position $(-y+\frac{1}{2}, x+\frac{1}{2}, z+\frac{3}{4})$.

Orientation error (°)	(*a*) *TFSGEN*	(*b*) *PTF*
0	22.0 (1.6) 1	12.5 (2.3) 1
3	15.1 (1.5) 1	8.6 (1.7) 1
6	8.5 (1.5) 1	5.0 (1.0) 1
9	4.9 (1.0) 1	3.8 (0.8) 7

we subjected the variable dimer of D1.3 in the complex FabE225-FabD1.3 to increasing deviations in one of the Eulerian angles, each time calculating the reciprocal-space PTF with both isomorphous phases and calculated phases (phasing with one molecule and searching with a symmetry-related component), and direct space PTF (*RTRANS*), the correlation coefficient search (*SEARCH*) and the Patterson-based search (*TFSGEN*). All translation functions were calculated at 3.5 Å resolution except the PTF with isomorphous phases, which was calculated to 4.0 Å. The results of these trials are given in Table 5. The search with *TFSGEN* was the most sensitive to error for this example; the correct peak was the maximum only when the orientation was less than 6-8° in error. By comparison, the PTF calculated with isomorphous phases proved to be the most robust since the correct peak remained the maximum until the error exceeded 12-14°. The reciprocal-space PTF using calculated phases and the correlation-coefficient search gave results of comparable quality although with the latter being marginally superior for this particular example; the correct peak persisted as being maximum up to an error of 10-12° in orientation. The PTF using *RTRANS* gave results only slightly better than *TFSGEN*; we find no obvious explanation for why *RTRANS* performed worse than the reciprocal-space protocol in this case. The difference in performance of the PTF when using calculated and isomorphous phases arises from the fact that, in the former case, both ρ and ρ_{model} in (1) are influenced by errors in the model while, in the latter, only ρ_{model} is affected. In contrast to FabD1.3-FabE225, trials with FvD1.3 showed that *TFSGEN* was more robust to orientation errors than the reciprocal-space PTF (see Table 6), suggesting that the performance of a particular translation function may be influenced more by the example (the data and the model) than the method.

5. Discussion

The PTF has not been widely used in the molecular replacement technique (see §2). The object of this paper has been to demonstrate its versatility and to describe the conditions which, in our experience, have given the best results. Since most of the necessary elements of software, such as structure-factor calculation and Fourier transformation routines, exist in the normal repertoire of programs used by crystallographers, the PTF may be readily included as an independent approach to solving the translation problem.

In all trials reported here, the PTF performed best when carried out at high resolution, whether with isomorphous or calculated phases. Removal of density from the phasing model is essential when calculated phases are used, since its dominating effect in the Fourier maps would otherwise lead to large spurious peaks. Masking by molecular envelopes gave cleaner results than did subtraction by using difference coefficients, especially when the phasing component was a small fraction of the unit-cell contents. When using difference coefficients, we consistently found that equating $\langle F_{obs} \rangle$ to $\langle F_{calc} \rangle$ as a function of resolution gave the best performance, in spite of there being only a small fraction of the crystal structure contributing to F_{calc}. Calculation times proved to be modest: a complete run with FvD1.3 took about 200 s on a VAX Station 3500 for both the difference coefficient and masking protocol (Fig. 1). Removal of density corresponding to known portions of the crystal structure was not necessary when isomorphous phases were used, and this has also been the experience of other researchers. In difficult cases, however, there may be an advantage in removing density from those components already placed in maps phased by isomorphous replacement.

In the case of FvD1.3, the use of full symmetry in the PTF, whether in direct or reciprocal space, proved not to be as good as when each symmetry position was used individually in the reciprocal-space procedure. Indeed, the results published by Cygler & Desrochers (1989) indicate that combining all symmetry positions in their direct-space procedure need

not always give a result superior to that where each symmetry is considered separately. We have found no clear explanation for this behaviour.

Our experience shows that the reciprocal-space PTF appears comparable in performance to other methods tried, namely, those provided by the programs *RTRANS*, *TFSGEN* and *SEARCH*. This conclusion is based on the S/N-ratio discrimination and in robustness to errors in orientation of the search model. The performance of a given translation function probably depends greatly on the influence of the particular errors on the diffraction data and the model. Thus, for a particular structure, one method may perform significantly better than the others and it is worth exploiting all possibilities. For example, the reciprocal-space PTF performed better than *TFSGEN* for FvD1.3 when the complete variable dimer was used as search model, while the reverse proved to be the case when only the V_L domain was used, even though the same observed structure amplitudes were employed [see § 4.1(ii)].

The structural examples we have discussed in this paper have concerned mainly Fab molecules, where one problem has been to locate the flexible variable and constant domains correctly with respect to one another in the unit cell. Two recent reports have shown how correlation between observed and model intensities (Yeates & Rini, 1990) or squared normalized structure amplitudes (Brünger, 1990) may be used to refine the relative orientations and translations within a flexible domain structure such as an Fab. This is referred to as Patterson correlation (PC) refinement. A separate translation search must, of course, be made to place the molecule in the unit cell. This method is very useful when the relative orientation and translation of either V_L and V_H of the variable dimer or C_L and C_H1 of the constant dimer are too much in error to produce an identifiable signal in the rotation function. The range of convergence of the PC method (Brünger, Leahy, Hynes & Fox, 1991) probably corresponds to the observed spread in angular and translational differences in the domain structure of variable dimers (Lascombe *et al.*, 1989). It may happen, however, that the relative orientation of the variable and constant dimers (defined as the elbow angle) of the search Fab model is very different in the unknown structure. A case in point is FabD1.3 where this angle is 172° in the complex with lysozyme and 138° in the complex with FabE225. The necessity to use several search models with elbow angles spaced systematically at suitable intervals could involve a lengthy calculation. PC refinement performed on the variable and constant dimers separately, however, may be sufficient to provide models that lead to successful translation searches for each of these components independently since we have found little difficulty in dealing with structures having four Fabs in the unit cell.

One additional use of the PTF which we have not tried here is to use the method to locate sets of heavy-atom coordinates from several isomorphous derivatives relative to the same crystallographic origin and the same enantiomorphic hand. This could prove particularly useful for polar space groups in which the patterns of heavy-atom substitution are complicated. If $\mathbf{F}_P$ is the native structure amplitude, $\mathbf{F}_{HP1}$ is the structure amplitude of derivative 1, $\mathbf{F}_{H1}$ is the calculated heavy-atom structure factor of derivative 1 and α_{P2} is the native protein phase calculated using the derivative 2 only, then the Fourier transform of

$$[\mathbf{F}_{HP1}(\mathbf{h}) - \mathbf{F}_P(\mathbf{h})] \exp [i\alpha_{P2}(\mathbf{h})] \cdot \mathbf{F}_{H1}(\mathbf{h})^*$$

would give a peak corresponding to the translation required to bring the heavy-atom positions of derivative 1 to the same origin as derivative 2, provided the choice of enantiomorphic hand is compatible. Unlike the procedures suggested by Rossmann (1960) and Kartha & Parthasarathy (1965), which use the correlation between two Patterson functions, the PTF gives the result as a single vector rather than as a complicated set of cross-vectors between the two sets of heavy-atom structures.

The PTF provides a simple means for referring independent fragments or molecules in the asymmetric unit to a common origin and this is probably the most useful aspect of the function. It is particularly efficient at this task since such a search must be made over the whole unit cell; unlike the *R*-factor (or correlation-coefficient) search, the calculation is not demanding in CPU time. An advantage not to be overlooked is that it offers an alternative to other translation functions. Thus, difficult cases in molecular replacement may benefit greatly by the correlation of results obtained by two or more independent translation functions.

Note added in proof: Since this article went to press, a publication by Driessen, Bax, Slingsby, Lindley, Mahadevan, Moss & Tickle (1991) has appeared which also draws attention to the similarity between the phased translation function and Patterson-based methods.

We are greatly indebted to Dr Jorge Navaza for invaluable discussions and, in particular, for suggesting the formulation of the full-symmetry PTF in reciprocal space.

References

AMIT, A. G., MARIUZZA, R. A., PHILLIPS, S. E. V. & POLJAK, R. J. (1986). *Science*, **233**, 747-753.

BENTLEY, G. A., BOULOT, G., RIOTTOT, M. M. & POLJAK, R. J. (1990). *Nature (London)*, **348**, 254-257.

BHAT, T. N., BENTLEY, G. A., FISCHMANN, T. O., BOULOT, G. & POLJAK, R. J. (1990). *Nature (London)*, **347**, 483-485.

BOULOT, G., EISELÉ, J. L., BENTLEY, G. A., BHAT, T. N., WARD, E. S., WINTER, G. & POLJAK, R. J. (1990). *J. Mol. Biol.* **213**, 617-619.

BOULOT, G., ROJAS, C., BENTLEY, G. A., POLJAK, R. J., BARBIER, E., LE GUERN, C & CAZENAVE, P. A. (1987). *J. Mol. Biol.* **194**, 577-578.
BRÜNGER, A. T. (1990). *Acta Cryst.* A**46**, 46-57.
BRÜNGER, A. T., LEAHY, D. J., HYNES, T. R. & FOX, R. O. (1991). *J. Mol. Biol.* **221**, 239-256.
COLMAN, P. M., DEISENHOFER, J., HUBER, R. & PALM, W. (1976). *J. Mol. Biol.* **100**, 257-282.
COLMAN, P. M., FEHLHAMMER, H. & BARTELS, K. (1976). In *Crystallographic Computing Techniques*, edited by F. R. AHMED, K. HUML & B. SEDLÁČEK, pp. 248-258. Copenhagen: Munksgaard.
CROWTHER, R. A. (1972). In *The Molecular Replacement Method*, edited by M. G. ROSSMANN, pp. 173-178. New York: Gordon & Breach.
CROWTHER, R. A. & BLOW, D. M. (1967). *Acta Cryst.* **23**, 544-548.
CYGLER, M. & ANDERSON, W. F. (1988*a*). *Acta Cryst.* A**44**, 38-45.
CYGLER, M. & ANDERSON, W. F. (1988*b*). *Acta Cryst.* A**44**, 300-308.
CYGLER, M. & DESROCHERS, M. (1989). *Acta Cryst.* A**45**, 563-572.
DOESBURG, H. M. & BEURSKENS, P. T. (1983). *Acta Cryst.* A**39**, 368-376.
DRIESSEN, H. P. C., BAX, B., SLINGSBY, C., LINDLEY, P. F., MAHADEVAN, D., MOSS, D. S. & TICKLE, I. J. (1991). *Acta Cryst.* B**47**, 987-997.
FISCHMANN, T. O., BENTLEY, G. A., BHAT, T. N., BOULOT, G., MARIUZZA, R. A., PHILLIPS, S. E. V., TELLO, D. & POLJAK, R. J. (1991). *J. Biol. Chem.* **266**, 12915-12920.
FUJINAGA, M. & READ, R. J., (1987). *J. Appl. Cryst.* **20**, 517-521.
HARADA, Y., LIFCHITZ, A., BERTHOU, J. & JOLLES, P. (1981). *Acta Cryst.* A**37**, 398-406.
HUBER, R. (1965). *Acta Cryst.* **19**, 353-356.
International Tables for X-ray Crystallography (1974). Vol. I. Birmingham: Kynoch Press.
KARTHA, G. & PARTHASARATHY, R. (1965). *Acta Cryst.* **18**, 749-753.
LASCOMBE, M. B., ALZARI, M., BOULOT, G., SALUDJIAN, P., TOUGARD, P., BEREK, C., HABA, S., ROSEN, E. M., NICONHOF, A. & POLJAK, R. J. (1989). *Proc. Natl Acad. Sci. USA*, **86**, 607-611.
NAVAZA, J. (1987). *Acta Cryst.* A**43**, 645-653.
READ, R. J. (1986). *Acta Cryst.* A**42**, 140-149.
READ, R. J. & SHIERBEEK, A. J. (1988). *J. Appl. Cryst.* **21**, 490-495.
ROSSMANN, M. G. (1960). *Acta Cryst.* **13**, 221-226.
ROSSMANN, M. G. & BLOW, D. M. (1962). *Acta Cryst.* **15**, 24-31.
SCHIERBEEK, A. J., SWARTE, M. B. A., DIJKSTRA, B. W., VRIEND, G., READ, R. J., HOL, W. G. J. & DRENTH, J. (1989). *J. Mol. Biol.* **206**, 365-379.
SERC Daresbury Laboratory (1986). *CCP4. A Suite of Programs for Protein Crystallography.* SERC Daresbury Laboratory, Warrington, England.
TAYLOR, C. A. & MORLEY, K. A. (1959). *Acta Cryst.* **12**, 101-105.
TICKLE, I. J. (1985). In *Molecular Replacement. Proceedings of the Daresbury Study Weekend*, 15-16 *February* 1985, edited by P. A. MACHIN, pp. 22-26.
YEATES, T. O. & RINI, J. M. (1990). *Acta Cryst.* A**46**, 352-359.

Acta Cryst. (1992). A**48**, 322-328

$(p2, 2^l)$-Symmetry Three-Dimensional Space Groups $G_3^{l,p2}$

BY S. V. JABLAN

The Mathematical Institute, Knez Mihajlova 35, *Belgrade, Yugoslavia*

(*Received* 29 *April* 1991; *accepted* 15 *November* 1991)

Abstract

By use of the antisymmetric characteristic method, $(p2, 2^l)$-symmetry three-dimensional space groups $G_3^{l,p2}$ $(p = 3, 4, 6)$ are derived.

Introduction

Crystallographic $(p2)$-symmetry three-dimensional space groups G_3^{p2} $(p = 3, 4, 6)$ were derived by Karpova (1980*a*, 1980*b*), Chubarova (1983) and Zamorzaev, Karpova, Lungu & Palistrant (1986). From 73 symmorphic space groups G_3 were derived 1025 junior G_3^{p2} (96 G_3^{32}+438 G_3^{42}+491 G_3^{62}), from 54 hemisymmorphic G_3, 945 junior G_3^{p2} (75 G_3^{32}+444 G_3^{42}+426 G_3^{62}) were derived and from 103 asymmorphic G_3, 1650 junior G_3^{p2} (138 G_3^{32}+785 G_3^{42}+727 G_3^{62}) were derived. Thus the category G_3^{p2} $(p = 3, 4, 6)$ consists of 3620 junior groups (309 G_3^{32}+1667 G_3^{42} 1644 G_3^{62}). By the use of the generalized antisymmetric characteristic method (AC method) introduced by the author (Jablan, 1990, 1991), some of these results will be corrected and all the crystallographic space groups of colour multiple antisymmetry $G_3^{l,p2}$ $(p = 3, 4, 6)$ will be derived.

1. Some general remarks on $(p2)$ and $(p2, 2^l)$ symmetry

$(p2)$ symmetry is a particular case of general P symmetry with $P = D_p$, where D_p is the irregular dihedral permutation group, generated by the permutations $e_1 = 1, \ldots, p$ and $e_2 = (2\,p), \ldots, ([(p+1)/2]\,p - [(p+1)/2]+2)$ $(p \geq 3)$, satisfying the relations

$$e_1^p = e_2^2 = (e_1 e_2)^2 = E.$$

For $p = 4q+2$ $(q \in N)$, the group D_p is reducible, so the relationship

$$D_{4q+2} \simeq \{e_1^2, e_2\} \times \{e_1^{2q+1}\} = D_{2q+1} \times C_2$$

holds, where $\{e_1^2, e_2\}$ and $\{e_1^{2q+1}\}$ denote, respectively,

0108-7673/92/030322-07$03.00